

Experimental and Clinical Endocrinology & Diabetes

Protective role of MerTK in diabetic peripheral neuropathy via inhibition of the NF- κ B signaling pathway

Xiaoyang Su, Wenting Chen, Yidan Fu, Bian Wu, Fugang Mao, Yan Zhao, Qiuping Yang, Danfeng Lan.

Affiliations below.

DOI: 10.1055/a-2301-3970

Please cite this article as: Su X, Chen W, Fu Y et al. Protective role of MerTK in diabetic peripheral neuropathy via inhibition of the NF- κ B signaling pathway. *Experimental and Clinical Endocrinology & Diabetes* 2024. doi: 10.1055/a-2301-3970

Conflict of Interest: The authors declare that they have no conflict of interest.

This study was supported by National Natural Science Foundation of China (<http://dx.doi.org/10.13039/501100001809>), 81860105, the Yunnan Key Laboratory of Innovative Application of Traditional Chinese Medicine, 202105AG070032, the Yunnan Health Training Project of High Level Talents, YNWR-QNBJ-2020-236, the Special Joint Program of Yunnan Province, 202001AY070001-159

Abstract:

Diabetic peripheral neuropathy impacts patient quality of life. Increased Mer tyrosine kinase expression has been demonstrated in such patients, yet its mechanism remains unclear. This study established type 2 diabetes mellitus and diabetic peripheral neuropathy models in Sprague Dawley rats via low-dose streptozotocin and a high-fat diet. Mer tyrosine kinase-specific inhibitors were administered by gavage once daily for 2 weeks. Sciatic nerve conduction velocity and nerve structure were measured. The levels of Mer tyrosine kinase, nuclear factor kappa-light-chain-enhancer of activated B cells, tumor necrosis factor-alpha, interleukin-1 beta, and relevant biochemical indexes were detected. The study revealed Mer tyrosine kinase upregulation in type 2 diabetes mellitus and more so in diabetic peripheral neuropathy groups. Inhibiting Mer tyrosine kinase led to reduced nerve conduction velocity and further deterioration of sciatic nerve structure, as evidenced by structural morphology. Concurrently, serum levels of total cholesterol, glycated hemoglobin, and triglyceride significantly rose. Moreover, nuclear factor kappa-light-chain-enhancer of activated B cells levels increased in both serum and nerve tissue, alongside a significant rise in tumor necrosis factor-alpha and interleukin-1 beta expressions. Mer tyrosine kinase was found to bind to inhibitor of kappa B kinase beta in Schwann cells, establishing inhibitor of kappa B kinase beta as a precursor to nuclear factor kappa-light-chain-enhancer of activated B cells activation. Inhibition of Mer tyrosine kinase exacerbates neuropathy, indicating its protective role in diabetic peripheral neuropathy by suppressing the nuclear factor kappa-light-chain-enhancer of activated B cells pathway, highlighting a potential new target for its diagnosis and treatment.

Corresponding Author:

Dr. Danfeng Lan, First People's Hospital of Yunnan Province, Kunming 650032, Yunnan, China, 650032 Yunnan, China, ang778@live.cn

Affiliations:

Xiaoyang Su, First Affiliated Hospital of Kunming Medical University, Kunming, China
Wenting Chen, First Affiliated Hospital of Kunming Medical University, Kunming, China
Yidan Fu, First Affiliated Hospital of Kunming Medical University, Kunming, China
[...]

Danfeng Lan, First People's Hospital of Yunnan Province, Yunnan, China

1Protective role of MerTK in diabetic peripheral neuropathy via inhibition of the NF- κ B signaling pathway

3Xiaoyang Su^{1#}, Wenting Chen², Yidan Fu², Bian Wu³, Fugang Mao⁴, Yan Zhao², Qiuping Yang², Danfeng Lan^{5*}

5¹Department of Critical Care Medicine, The First Affiliated Hospital of Kunming Medical University, Kunming 650032, Yunnan, P.R. China

7²Department of Endocrinology, The First Affiliated Hospital of Kunming Medical University, Kunming 650032, Yunnan, P.R. China

9³Department of General Surgery II, The First People's Hospital of Yunnan Province, Yunnan
10Key Laboratory of Innovative Application of Traditional Chinese Medicine, Kunming
11650032, Yunnan, China

12⁴Department of Ultrasound, The First People's Hospital of Yunnan Province, The Affiliated
13Hospital of Kunming University of Science and Technology, Kunming 650032, Yunnan,
14China

15⁵Department of Gastroenterology, The First People's Hospital of Yunnan Province, Yunnan
16Digestive Disease Clinical Medical Center, Kunming 650032, Yunnan, China

17*Correspondence should be addressed to Danfeng Lan (ang778@live.cn)

18

19Abstract

20Diabetic peripheral neuropathy impacts patient quality of life. Increased Mer tyrosine kinase
21expression has been demonstrated in such patients, yet its mechanism remains unclear. This
22study established type 2 diabetes mellitus and diabetic peripheral neuropathy models in
23Sprague Dawley rats via low-dose streptozotocin and a high-fat diet. Mer tyrosine kinase-
24specific inhibitors were administered by gavage once daily for 2 weeks. Sciatic nerve
25conduction velocity and nerve structure were measured. The levels of Mer tyrosine kinase,
26nuclear factor kappa-light-chain-enhancer of activated B cells, tumor necrosis factor-alpha,
27interleukin-1 beta, and relevant biochemical indexes were detected. The study revealed Mer

28tyrosine kinase upregulation in type 2 diabetes mellitus and more so in diabetic peripheral
29neuropathy groups. Inhibiting Mer tyrosine kinase led to reduced nerve conduction velocity
30and further deterioration of sciatic nerve structure, as evidenced by structural morphology.
31Concurrently, serum levels of total cholesterol, glycated hemoglobin, and triglyceride
32significantly rose. Moreover, nuclear factor kappa-light-chain-enhancer of activated B cells
33levels increased in both serum and nerve tissue, alongside a significant rise in tumor necrosis
34factor-alpha and interleukin-1 beta expressions. Mer tyrosine kinase was found to bind to
35inhibitor of kappa B kinase beta in Schwann cells, establishing inhibitor of kappa B kinase
36beta as a precursor to nuclear factor kappa-light-chain-enhancer of activated B cells
37activation. Inhibition of Mer tyrosine kinase exacerbates neuropathy, indicating its protective
38role in diabetic peripheral neuropathy by suppressing the nuclear factor kappa-light-chain-
39enhancer of activated B cells pathway, highlighting a potential new target for its diagnosis
40and treatment.

41**Key words:** diabetic peripheral neuropathy; MerTK; NF-kb signaling pathway; inflammatory
42factors; protective effect

431. Introduction

44Diabetes mellitus (DM) is a chronic metabolic disorder with increasing incidence in
45developing countries, representing a global health concern. Its prevalence is estimated to
46reach 642 million by 2040 [1,2]. Patients with diabetes usually present a series of
47macrovascular and microvascular complications, such as ischemic heart disease, nephropathy,
48retinopathy, and neuropathy [3,4]. In addition to disease duration and glucose control, genetic
49background may influence diabetic complications [5]. Diabetic neuropathy (DN) is a
50syndrome characterized by central and peripheral nervous system lesions caused by chronic
51hyperglycemia; notably, it is one of the most common diabetic target organ damages that can
52occur in both patients with type 1 DM and those with type 2 DM (T2DM) [6]. Moreover,
53diabetic peripheral neuropathy (DPN) is a major type of DN with an incidence of 58.5% in
54patients with diabetes and a high mortality rate, which severely impairs the quality of life of
55patients [7,8]. However, the clinical onset of DPN is often severe, and disease development is
56relatively long [9]. The early diagnosis of DPN is challenging. Thus, studying the
57pathogenesis and identifying early biomarkers of DPN will contribute to the effective
58prediction and intervention of DPN progression.

59 In our previous studies, we reported that Mer Tyrosine Kinase (MerTK) levels were
60significantly increased both in the peripheral blood of patients with DPN and in the sciatic
61nerve of early DPN mice, suggesting that changes in MerTK gene expression may be a
62potential biomarker for the early diagnosis of DPN [10]. Specifically, MerTK is a member of
63the MER/AXL/TYRO3 tyrosine receptor kinase family, is involved in cell phagocytosis, and
64encodes a transmembrane protein that is distributed on the surface of various specific and
65non-specific phagocytic cells, such as retinal pigment epithelial cells, macrophages, and
66dendritic cells [11]. Recently, studies have suggested that Nuclear Factor kappa-light-chain-

67enhancer of activated B cells (NF- κ b) was implicated in the pathophysiological mechanism of
68DPN [12,13]. NF- κ b is an important precursor of proinflammatory factor and a heterodimer
69composed of p65 (RelA) and p50 [14]. The formation of DPN is commonly attributed to
70endothelial cell activation and inflammatory gene induction, regulated centrally by the
71transcription factor NF- κ b [15,16]. Previous studies have found that the MER/AXL/TYRO3
72family was associated with the NF- κ b pathway [17], and MerTK could alleviate
73staphylococcal lipophosphate-induced inflammatory response by blocking NF- κ b activation
74[18]. Therefore, we speculate that MerTK may influence the development of DPN by
75regulating the NF- κ b signaling pathway.

76 To simulate the disease characteristics of T2DM progressing to DPN, a high-sugar and -
77fat diet combined with a low-dose streptozotocin (STZ) injection was used to create a T2DM
78animal model in Sprague Dawley (SD) rats. The DPN model was constructed by
79continuously feeding a high-sugar and high-fat diet for 8 weeks. We focused on the
80administration of MerTK-specific inhibitors MRX-2843, the conduction velocity and
81structural changes of the sciatic nerve, and the levels of MerTK, NF- κ b, Tumor Necrosis
82Factor (TNF)- α , interleukin (IL)-1 β , and relevant biochemical indexes. Our study aimed to
83determine the regulatory role of MerTK in the NF- κ b signaling pathway and its effect on the
84pathogenesis of DPN to provide a new biomarker for the early prediction of DPN as well as
85an effective therapeutic target for the treatment of DPN.

86

872. Materials and methods

882.1 Animal studies

89All experiments were performed with the approval of the Animal Experimentation
90Committee of Kunming Medical University and in accordance with the institutional
91regulations (No. kmmu20221595). Overall, 70 8-week-old SD rats (310–350 g) from
92Kunming Medical University's Animal Center (No. 2019-0004) were divided into 5 groups,
93with 14 rats per group. The control (CON) group received an ordinary diet and 0.2 mL of
940.9% normal saline (NS) by gavage daily. The CON+ MRX-2843 group was similarly fed but
95received a 0.2 mL 65 mg/kg MRX-2843 suspension daily for 2 weeks. The T2DM group was
96fed a high-fat and -sugar diet for 6 weeks, then injected with a 1.5 mL solution of STZ (35
97mg/kg) to induce diabetes. Blood glucose levels were measured on days 3, 7, and 14 post-
98STZ administration; levels ≥ 16.7 mmol/L indicated successful T2DM modeling. Rats then
99received an ordinary diet and 0.2 mL 0.9% NS gavage daily. For the DPN group, post-T2DM
100establishment, rats were switched to a high-fat and -sugar diet for 8 weeks, followed by an
101ordinary diet and daily 0.2 mL 0.9% NS gavage. In the DPN+ MRX-2843 group, post-DPN
102establishment, a 65-mg/kg MRX-2843 suspension was administered daily for 2 weeks.

103

1042.2 Detection of sciatic nerve conduction velocity (NCV)

105Based on the body weight and status of the rats, 0.9% pentobarbital sodium (30 mg/kg) was
106injected intraperitoneally, the sciatic nerve was isolated and the NCV was detected. The
107double-stimulation needle electrode was placed at the left sciatic notch, and the recording
108electrode was placed between the second toe of the right plantar. The reference electrode was
109placed between the stimulation electrode and the recording electrode, approximately 1 cm
110away from the recording electrode. The intensity of the stimulation was gradually increased

111from a small value, and the measured electromiography was recorded over time. NCV was
112indicated according to the ratio of latency to conduction distance of compound action
113potential, calculated by dividing the distance between the stimulation electrode and the
114recording electrode by the difference obtained from the proximal latency minus the distal
115latency and expressed in meters per second. The Biological Function Experimental System
116was provided by the Biological Function Laboratory of the Kunming Medical University.
117Sciatic NCV measurement under <40 m/s indicated successful DPN modeling [19].

118

1192.3 Detection of blood biochemical indexes

120Blood was collected from the hearts of rats after execution, separated at 2795 G for 15 min at
1214 °C, and the upper plasma was obtained after stratification. Blood glucose, triglyceride
122(TG), and total cholesterol (TC) levels were measured using a biochemical analyzer (BS-
123240VET, Shenzhen Mairad Company). Insulin (INS) and glycated hemoglobin (GHB)
124levels were measured using enzyme-linked immunosorbent assay (ELISA) kits (INS:
125Elabscience Item, No. E-EL-R2466; GHB: Mlbio Item, No. ml059468).

126

1272.4 ELISA

128The levels of MerTK, NF- κ b (P65), TNF- α , and IL-1 β in the serum were determined by the
129double antibody sandwich method. Purified rat antibodies were coated onto each microwell
130plate to prepare solid-phase antibodies, added to the corresponding coated microwell, and
131combined with horseradish peroxidase (HRP)-labeled antibodies. The antibody-antigen-
132enzyme-labeled antibody complex was formed, and tetramethylbenzidine (TMB) substrate

133was added for color development after thorough washing. TMB was transformed into blue
134under the catalysis of the HRP enzyme and into yellow under the action of an acid.
135Absorbance (OD value) was measured at 450 nm using a microplate reader to calculate the
136concentrations of MerTK, NF- κ b (P65), TNF- α , and IL-1 β in samples via standard curves
137from ELISA kits (MerTK: Thermo Fisher, EHMER; NF- κ b(P65): Elabscience, E-EL-R0674;
138TNF- α : Elabscience, E-EL-R2856; IL-1 β : Elabscience, E-EL-R0012).

139

1402.5 Detection of sciatic nerve histopathology

141The sciatic nerve was fixed in 10% buffered formaldehyde. The fixed tissues were soaked in
142alcohol for dehydration and placed in dimethylbenzene. The tissue was soaked and permeated
143in paraffin, and the paraffin-embedded tissue was sliced into about 5- μ m-thick slices. The
144tissue was baked at 60 °C in an incubator for 30 min. The tissues were then hydrated.
145Hematoxylin-eosin (HE) staining was performed using hematoxylin for 10–20 min. After
146rinsing with water, the solution was placed in a weakly alkaline aqueous solution and turned
147blue until blue appeared. Next, 85% alcohol was added for 3–5 min, followed by staining
148with eosin for 3–5 min. The toluidine blue (TB)-stained section was incubated in 1%
149toluidine blue aqueous solution at 50 °C, then at 56 °C for 20 min. After rinsing, samples
150were immersed in 70% alcohol for 1 min, dehydrated, sealed, and examined under a light
151microscope.

152

1532.6 Observation by electron microscopy

154Sciatic nerve tissue, approximately 1 mm thick, was treated with 4% glutaraldehyde for pre-

155fixation and 1% acid for post fixation. After rinsing with PBS, the sections were dehydrated
156with acetone, embedded in epoxy resin, sliced using an ultrathin slicer, stained with uranium
157acetate and lead citrate solution in a box, and observed and photographed using a
158transmission electron microscope (JEM-1400).

159

1602.7 Immunohistochemistry

161The sciatic nerve was fixed in 10% buffered formaldehyde, dehydrated using an ethanol
162gradient, embedded in paraffin, and sliced. The sections were immersed in citrate buffer (PH
1636.0) for repair and then cleaned with PBS. The slices were then treated with a buffer-blocking
164solution (5% goat serum). The blocking solution of goat serum was added, and the first
165antibody of MerTK (1:100, Affinity, USA) and NF- κ b (1:100, Affinity, USA) was added. The
166glass slides were placed in a 4 °C refrigerator overnight. After rinsing with PBS, the sections
167were incubated with secondary antibodies, including goat anti-rabbit IgG (H+L) HRP (1:200,
168Affinity, USA) and goat anti-mouse IgG (H+L) HRP (1:200, Affinity, USA). DAB
169chromogen solution was added to terminate the staining. Finally, the experimental results
170were observed under an optical microscope, and the brown or brown-yellow particles in the
171cell membrane or cytoplasm were considered protein expression. Four fields from each
172section were randomly selected under a microscope.

173

1742.8 Immunofluorescence staining

175The sciatic nerve was fixed in 10% buffered formaldehyde, dehydrated using an ethanol
176gradient, embedded in paraffin, and sliced. The sections were then immersed in a citrate

177buffer (PH 6.0) for repair. Goat serum was added to the blocking solution, and the primary
178antibody against MerTK (Affinity: DF4785) was added. The glass slides were put in a wet
179box and placed in a 4 °C refrigerator overnight. After rinsing with PBS buffer, the slices were
180added with the second antibodies of goat anti-rabbit IgG (H+L) HRP (1:200, Affinity, USA)
181and treated at 37 °C for 30 min. After washing with PBS three times, DAPI was dropped and
182incubated at room temperature for 10 min. After rinsing with PBS, the slices were sealed with
183anti-fluorescence attenuating tablets. Finally, images were captured and observed by
184fluorescence microscopy.

185

1862.9 Western blotting analysis

187Total protein was extracted using RIPA buffer (Beyotime Biotechnology, China), isolated by
188SDS-polyacrylamide gel electrophoresis (SDS-PAGE), and transferred to a polyvinylidene
189fluoride membrane (Millipore ISEQ00010). Subsequently, the membranes were incubated
190with primary antibody (1:1000 for anti-MerTK □ Abcam, ab52981; 1:1000 for anti-NF-κb,
191Proteintech, 80979-1-RR; 1:3000 for anti-TNF-α, Proteintech, 60291-1-Ig; 1:3000 for anti-β-
192actin, Proteintech, 81115-1-RR) and kept at 4 °C overnight. Detection was performed using a
193horseradish peroxidase secondary antibody (goat anti-mouse IgG[H+L] HRP, 1:3000,
194Affinity, USA) after incubation at room temperature for 2h. Subsequently, protein expression
195was visualized using an ECL kit and an X-ray film. Membranes displayed luminescence
196using a Bio-Rad luminescence imaging system.

197

1982.10 Immunoprecipitation (co-ip) assays

199The interaction of endogenous MerTK and Ikbkb was detected by the co-ip assays using
200RSC96 cells. RSC96 cells were lysed and centrifuged. The input protein was retained, and
201MerTK, Ikbkb, and IgG primary antibodies were added to the resulting product. After
202overnight incubation at 4 °C, 5 µL Protein A and Protein G were added and then incubated,
203washed, and centrifuged. Following incubation, washing, centrifugation, resuspension in SDS
204buffer, and denaturation, the final product was obtained, and finally, the interaction between
205MerTK and Ikbkb was detected by immunoblotting. An immunoprecipitation kit was
206purchased from Shanghai Ebixin Technology Co.

207

2082.11 Statistical analysis

209All experiments were performed at least three times. Data are expressed as the mean ± SD. A
210normality test was performed to determine normal distribution. Student t-test was used to
211compare the means between two groups, while the data among multiple groups were
212analyzed using one-way analysis of variance followed by the "Tukey or Dunnet post hoc"
213test. All statistical analyses were performed using SPSS 22.0 software. Statistical significance
214was defined as a P-value <0.05.

215

2163. Results

2173.1 Model of DPN rats was established successfully, and the NCV was decreased after 218inhibiting MerTK

219Rats fed a high-fat and -sugar diet combined with STZ injections exhibited typical symptoms
220of T2DM, such as hyperglycemia, polyuria, polydipsia, polyphagia, and weight loss. The
221DPN rat model was established by continuously feeding rats high-fat and -sugar diets and

222was confirmed by blood glucose detection and electrophysiological experiments. After 8
223weeks of continued high-fat and -sugar feeding, diabetic rats exhibited significantly lower
224body weights and higher blood glucose levels than did non-diabetic rats. MRX-2843 had no
225significant influence on the body weight or blood glucose levels in the inhibitor group
226(**Figure 1A, B**). Moreover, sciatic NCV was significantly reduced in the DPN group, and
227NCV was significantly lower in the DPN+MRX-2843 group than in the DPN group (**Figure**
228**1C**).

229

2303.2 Changes of MerTK expression in each group

231MerTK expression was detected in the longitudinal section of the sciatic nerve using
232immunofluorescence (**Figure 2**), immunohistochemistry (**Figure 3**), and western blotting
233(**Figure 4a**), and in the serum of rats using ELISA (**Figure 4b,c**). The results showed that
234MerTK expression was upregulated in both the T2DM and DPN groups and increased
235significantly in the DPN group than in the CON and T2DM groups. After the MerTK
236inhibitor MRX-2843 was administered, MerTK expression decreased significantly in the
237CON +MRX-2843 and DPN +MRX-2843 groups, indicating that the MerTK inhibitor
238effectively inhibited MerTK.

239

2403.3 Changes of INS, TC, GHB, and TG in each group

241INS, TC, GHB, and TG levels were notably higher in the DPN group than in the CON group,
242indicating the involvement of glucose and lipid metabolism disturbances and insulin
243resistance in DPN's development. Inhibiting MerTK expression significantly raised TC,
244GHB, and TG serum levels, exacerbating these metabolic disorders (**Figure 5**).

245

2463.4 Changes in structural morphology in the longitudinal sections of the sciatic nerve

247After HE staining, the sciatic nerves in the CON group showed that the medullated nerve

248 fibers were evenly distributed, continuous, complete, neat, and orderly, and the myelin
249 sheaths were regular in shape and densely arranged. In the DPN group, the nerve fibers were
250 arranged sparsely and chaotically, with irregular morphology and unclear borders. Some
251 axons were shrunken or lost, which was accompanied by demyelination and myelinolysis.
252 The structure of the medullated nerve fibers was disordered in cross-section, with axonal
253 swelling accompanied by axon shrinkage and partial demyelination. TB staining revealed that
254 the nerve fibers in the CON group were dense, the individual fibers were full, and the
255 thickness of the myelin sheath was uniform. In the DPN group, the nerve fibers were loose,
256 the myelin sheath was thin, and the axons were small and centrally located. After MerTK
257 inhibition, the structure of the nerve fibers was further disrupted, and the lesion worsened
258 **(Figure 6a)**.

259 Under an electron microscope, the sciatic nerve in the CON group exhibited evenly
260 arranged medullated nerve fibers, the structure of the myelin sheath was intact and dense, and
261 the morphology of Shewan's cells showed no obvious abnormalities. In the DPN group, the
262 shape of myelinated nerve fibers was irregular in cross-section, the myelin sheath was loose
263 and foveolar, some of the myelin sheaths were deformed and vacuolated, and microtubules
264 and microfilaments in axons were disturbed or had disappeared. The nuclei of Shewan cells
265 had an irregular morphology with dilated perinuclear gaps, and the nuclear membranes were
266 partially dissolved and ruptured. After MerTK inhibition, the looseness of the nerve fibers
267 was aggravated, axons were reduced, and lesions worsened **(Figure 6b)**.

268

269 **3.5 Expression of NF- κ b and downstream inflammatory factors was upregulated when** 270 **MerTK was inhibited**

271 The expression of NF- κ b (P65) was determined via immunohistochemistry **(Figure 7)**,
272 western blotting **(Figure 8)**, and ELISA **(Figure 9a)**. The inflammatory factors TNF- α and
273 IL-1 β were detected via western blotting **(Figure 8)** and ELISA **(Figure 9 (b and c))**,

274**respectively**). The results indicated upregulated expressions of P65, TNF- α , and IL-1 β in the
275DPN group, with further significant increases following MerTK inhibition, suggesting
276MerTK's protective role in DPN by inhibiting the NF- κ b pathway.

277

2783.6 MerTK bonded to I κ bb in Schwann cells

279Immunoprecipitation assays demonstrated specific binding between MerTK and I κ bb
280antibodies to their respective immunoprecipitates in RSC96 cells (**Figure 10A, B**). Western
281blot analysis revealed an increase in I κ bb expression concurrent with a decrease in MerTK
282expression (P <0.05) (**Figure 10C, D**). Immunofluorescence double staining indicated
283enhanced fluorescence of I κ bb (red) and P65 (green) following MerTK-siRNA3 interference
284(**Figure 10E**), highlighting MerTK's endogenous binding to I κ bb and its regulatory role in
285the NF- κ b signaling pathway.

286

2874. Discussion

288In this study, the T2DM model was established using high-sugar and -fat diets for 6 weeks
289combined with low-dose STZ injection in SD rats (35 mg/kg), which was considered a
290successful model when the blood glucose level was greater than 16.7 mmol/L. Based on the
291T2DM model, the rats were fed with high-sugar and -fat diets continuously for 8 weeks, and
292the DPN model was confirmed by detecting the blood biochemical index, sciatic nerve
293conduction velocity (NCV <40 m/s), and the morphology of the nerve structure, which is
294easy to generate and widely available for exploring behavioral or pharmacological tests
295associated with long-term diabetic complications as well as for studying the pathogenesis of
296diabetic complications.

297 MerTK is expressed in both immune and non-immune cells and is involved in
298inflammation, metabolism, and vascular homeostasis [20]. Previous studies have indicated
299that MerTK protects against liver fibrosis and cancer [21-23]. The expression of MerTK in

300the sciatic nerve and serum of rats was detected via immunohistochemistry,
301immunofluorescence, western blotting, and ELISA methods in our study, which showed that
302MerTK was upregulated in the T2DM and DPN groups, and the expression of MerTK was
303significantly increased in the DPN group than in the CON and T2DM groups, which is
304consistent with the results of our previous study [10]. After administering MerTK-specific
305inhibitors, sciatic nerve conduction velocity decreased, and structural disruption was
306observed, indicating DPN exacerbation upon MerTK inhibition and its protective role in DPN
307development. MerTK, a crucial tyrosine kinase, significantly influences PI3K/AKT and NF-
308 κ B pathway regulation and apoptotic cell-induced monocyte-derived dendritic cell inhibition
309[24, 25]. In addition, MerTK has been reported to affect organ function during inflammatory
310processes or any other injury, such as pathogen invasion [26].

311 In clinical studies, the levels of inflammatory markers have been shown to predict the
312onset and progression of diabetic complications [27]. NF- κ b is a protein complex that
313controls transcribed DNA, cytokine production, and cell survival; it is present in almost all
314animal cell types and is involved in cellular responses to stimuli. Moreover, it plays a key
315role in regulating the immune response to infections [28–29]. Previous studies have shown
316that the NF- κ b pathway-mediated inflammatory response played a central role in the
317pathogenesis of diabetes-related complications, including peripheral neuropathy. NF- κ b
318activation was involved in the insulin resistance and apoptosis of pancreatic β -cells [30].
319TNF- α and IL-1 β , the NF- κ b-mediated downstream inflammatory factors, play a central role
320in the inflammatory response, including immediate, acute, and chronic inflammation [31].
321Our studies showed NF- κ b (P65), TNF- α , and IL-1 β expressions were higher in the DPN
322group, further increasing with MerTK inhibition, indicating MerTK's protective effect in
323DPN by inhibiting the NF- κ b pathway. Additionally, MerTK influences metabolism-related
324indices by programming macrophages metabolically and epigenetically [24,32]. Here, the
325levels of TG, TC, and GHB increased significantly in the serum after MerTK inhibition,

326indicating the aggravation of blood glucose and lipid metabolism disorders.

327 To elucidate the MerTK-NF- κ b interaction, we identified Ikbkb (IKK β , IKK2), a
328catalytic subunit of the Ikb kinase complex and key NF- κ b pathway regulator, from the
329National Centre for Biotechnology Information. This complex swiftly activates NF- κ b,
330orchestrating target gene expression [33]. Diabetes induces Ikb phosphorylation and
331degradation, allowing P50 and P65 to signal the nucleus and activate genes that regulate
332DPN-associated pathophysiological changes [34]. We verified MerTK's endogenous
333interaction with Ikbkb in Ceibomb cells via immunoprecipitation. Interfering with MerTK
334increased Ikbkb expression, significantly enhancing Ikbkb and P65 immunofluorescence (P
335<0.05); this indicates that MerTK silencing upregulates Ikbkb, activating the NF- κ b pathway
336and P65 expression, thus suggesting MerTK's role in inflammation through NF- κ b signaling.

337 In summary, this study found that MerTK increased significantly in the DPN rats,
338neuropathy was aggravated, and inflammatory factors were upregulated when MerTK was
339inhibited. MerTK played a protective role in the progression of DPN by inhibiting the NF- κ b
340pathway. Our findings provide a valuable reference for studies on other diabetic
341complications owing to their similar pathogenesis and suggest that MerTK may be an early
342diagnostic marker and a new target for the treatment of DPN.

343

344**Acknowledgments**

345We thank Prof. Di Lu and Prof. Lechun Lv for their valuable discussions and technical
346assistance. We thank the scientific and technological achievements of the incubation center of
347Kunming Medical University for providing the experimental platform.

348**Authors contributions**

349Danfeng Lan, Qiuping Yang, and Yan Zhao constructed the concept of the study. Wenting
350Chen and Yidan Fu performed the experiments and wrote the manuscript. Bian Wu and
351Fugang Mao analyzed the results. Danfeng Lan and Qiuping Yang revised the manuscript. All

352the authors have read and approved the publication of the manuscript.

353Funding

354This work was supported by the National Natural Science Foundation of China (81860105),
355the Special Joint Program of Yunnan Province (202001AY070001-159, 202401AY070001-
356040), the Yunnan Youth Top Talent Project of High-Level Talents (YNWR-QNBJ-2020-236),
357the Yunnan Health Training Project of High-Level Talents Medical Reserve Talent Project
358(H-2019036), the Kunming University of Science and Technology, the First People's Hospital
359of Yunnan Province Joint Special Project on Medical Research (KUST- KH2022013Y), and
360the Yunnan Key Laboratory of Innovative Application of Traditional Chinese Medicine
361(202105AG070032).

362Conflict of Interest

363The authors declare no conflict of interest.

364

365References

3661. L'Heveder R, Nolan T. International diabetes federation. *Diabetes Res Clin Pract*, 2013;
367 101(3): 349-351.
3682. Tesfaye S, Selvarajah D. Advances in the epidemiology, pathogenesis and management of
369 diabetic peripheral neuropathy. *Diabetes Metab Res Rev*, 2012; 28 Suppl 1: 8-14.
3703. Lotfy M, Adeghate J, Kalasz H, et al. Chronic complications of diabetes mellitus: a mini
371 review. *Curr Diabetes Rev*, 2017; 13(1): 3-10.
3724. Tesfaye S, Selvarajah D, Gandhi R, et al. Diabetic peripheral neuropathy may not be as its
373 name suggests: evidence from magnetic resonance imaging. *Pain*, 2016; 157 Suppl 1:
374 S72-S80.
3755. Elzinga S E, Eid S A, McGregor B A, et al. Transcriptomic analysis of diabetic kidney

376 disease and neuropathy in mouse models of type 1 and type 2 diabetes. *Dis Model*
377 *Mech*, 2023; 16(10): dmm050080.

3786. Yu Y. Gold standard for diagnosis of dpn. *Front Endocrinol (Lausanne)*, 2021; 12: 719356.

3797. Iqbal Z, Azmi S, Yadav R, et al. Diabetic peripheral neuropathy: epidemiology, diagnosis,
380 and pharmacotherapy. *Clin Ther*, 2018; 40(6): 828-849.

3818. Tesfaye S, Boulton A J, Dyck P J, et al. Diabetic neuropathies: update on definitions,
382 diagnostic criteria, estimation of severity, and treatments. *Diabetes Care*, 2010; 33(10):
383 2285-2293.

3849. Sloan G, Alam U, Selvarajah D, et al. The treatment of painful diabetic neuropathy. *Curr*
385 *Diabetes Rev*, 2022; 18(5): e2001717820.

38610. Lan D, Jiang H Y, Su X, et al. Transcriptome-wide association study identifies
387 genetically dysregulated genes in diabetic neuropathy. *Comb Chem High Throughput*
388 *Screen*, 2021; 24(2): 319-325.

38911. Audo I, Mohand-Said S, Boulanger-Scemama E, et al. MERTK mutation update in inherited
390 retinal diseases. *Hum Mutat*, 2018; 39(7): 887-913.

39112. Yang J, Wei Y, Zhao T, et al. Magnolol effectively ameliorates diabetic peripheral
392 neuropathy in mice. *Phytomedicine*, 2022; 107: 154434.

39313. Feng Y, Chen L, Luo Q, et al. Involvement of miR-146a in diabetic peripheral
394 neuropathy through the regulation of inflammation. *Drug Des Devel Ther*, 2018; 12:
395 171-177.

39614. Ren C, Han X, Lu C, et al. Ubiquitination of NF- κ B p65 by FBXW2 suppresses breast cancer
397 stemness, tumorigenesis, and paclitaxel resistance. *Cell Death Differ*, 2022; 29(2): 381-
398 392.

39915. Perry B D, Caldwor M K, Brennan-Speranza T C, et al. Muscle atrophy in patients with
400 type 2 diabetes mellitus: roles of inflammatory pathways, physical activity and
401 exercise. *Exerc Immunol Rev*, 2016; 22: 94-109.
40216. Li J S, Ji T, Su S L, et al. Mulberry leaves ameliorate diabetes via regulating metabolic
403 profiling and ages/rage and p38 mapk/nf- κ b pathway. *J Ethnopharmacol*, 2022; 283:
404 114713.
40517. Korbecki J, Simińska D, Gąssowska-Dobrowolska M, et al. Chronic and cycling hypoxia:
406 drivers of cancer chronic inflammation through hif-1 and nf- κ b activation: a review of
407 the molecular mechanisms. *Int J Mol Sci*, 2021; 22(19).
40818. Shi X, Chen Y, Nadeem L, et al. Beneficial effect of TNF- α inhibition on diabetic
409 peripheral neuropathy. *J Neuroinflammation*, 2013; 10:6 9.
41019. Zahoor A, Yang C, Yang Y, et al. Mertk negatively regulates staphylococcus aureus
411 induced inflammatory response via socs1/socs3 and mal. *Immunobiology*, 2020;
412 225(4): 151960.
41320. Musso G, Cassader M, De Michieli F, et al. Mertk rs4374383 variant predicts incident
414 nonalcoholic fatty liver disease and diabetes: role of mononuclear cell activation and
415 adipokine response to dietary fat. *Hum Mol Genet*, 2017; 26(9): 1747-1758.
41621. Cai B, Dongiovanni P, Corey K E, et al. Macrophage mertk promotes liver fibrosis in
417 nonalcoholic steatohepatitis. *Cell Metab*, 2020; 31(2): 406-421.
41822. Huelse J M, Fridlyand D M, Earp S, et al. Mertk in cancer therapy: targeting the receptor
419 tyrosine kinase in tumor cells and the immune system. *Pharmacol Ther*, 2020; 213:
420 107577.
42123. Yan D, Huelse J M, Kireev D, et al. Mertk activation drives osimertinib resistance in

- 422 egfr-mutant non-small cell lung cancer. *J Clin Invest*, 2022; 132(15).
42324. Pipitone R M, Calvaruso V, Di Marco L, et al. Mer tyrosine kinase (merck) modulates
424 liver fibrosis progression and hepatocellular carcinoma development. *Front Immunol*,
425 2022; 13: 926236.
42625. Sen P, Wallet M A, Yi Z, et al. Apoptotic cells induce mer tyrosine kinase-dependent
427 blockade of nf-kappab activation in dendritic cells. *Blood*, 2007; 109(2): 653-660.
42826. Lin J, Xu A, Jin J, et al. MERTK-mediated efferocytosis promotes immune tolerance and
429 tumor progression in osteosarcoma through enhancing m2 polarization and pd-l1
430 expression. *Oncoimmunology*, 2022; 11(1): 2024941.
43127. Spranger J, Kroke A, Möhlig M, et al. Inflammatory cytokines and the risk to develop
432 type 2 diabetes: results of the prospective population-based european prospective
433 investigation into cancer and nutrition (epic)-potsdam study. *Diabetes*, 2003; 52(3):
434 812-817.
43528. Dolcet X, Llobet D, Pallares J, et al. Nf-kb in development and progression of human
436 cancer. *Virchows Arch*, 2005; 446(5): 475-482.
43729. Schlein L J, Thamm D H. Review: nf-kb activation in canine cancer. *Veterinary*
438 *Pathology*, 2022; 59(5): 724-732.
43930. He F, Huang Y, Song Z, et al. Mitophagy-mediated adipose inflammation contributes to
440 type 2 diabetes with hepatic insulin resistance. *J Exp Med*, 2021; 218(3).
44131. Olefsky J M, Glass C K. Macrophages, inflammation, and insulin resistance. *Annu Rev*
442 *Physiol*, 2010; 72: 219-246.
44332. Thai L M, O'Reilly L, Reibe-Pal S, et al. B-cell function is regulated by metabolic and
444 epigenetic programming of islet-associated macrophages, involving axl, merck, and

445 $\text{tgf}\beta$ receptor signaling. *iScience*, 2023; 26(4): 106477.

44633. Pai Y W, Lin C H, Lin S Y, et al. Reconfirmation of newly discovered risk factors of
447 diabetic peripheral neuropathy in patients with type 2 diabetes: A case-control study.
448 *PLoS One*, 2019;14(7):e220175.

44934. Mu Z P, Wang Y G, Li C Q, et al. Association Between Tumor Necrosis Factor- α and
450 Diabetic Peripheral Neuropathy in Patients with Type 2 Diabetes: a Meta-Analysis.
451 *Mol Neurobiol*, 2017; 54(2):983-996.

452

453

454

455

456

457

458

459 **Figure legends**

460 **Figure 1. Basic parameters of rats in each group.** (A) Changes in body weight in each
461 group at weeks 2, 4, 6, 8, 10, 12, 14, and 16. There were no significant changes in the body
462 weight of the rats after MerTK inhibition. (B) Changes in blood glucose levels in each group.
463 (C) Changes in sciatic NCV in each group at week 18. * $p < 0.05$. Group counts were as
464 follows: CON: 14; CON+MRX-2843: 14; T2DM: 10; DPN: 12; DPN+MRX-2843: 10. All
465 rats were aged 96 weeks.

466 **Figure 2. Immunofluorescence detection of MerTK expression in each group.** Confocal
467 images of MerTK (green) and DAPI (blue) staining of the nucleus. Scale bar = 500 μm (first
468 column). Scale bar = 50 μm (second, third, and fourth columns). Rat counts per group were:
469 CON: 14, CON+MRX-2843: 14, T2DM: 10, DPN: 12, DPN+MRX-2843: 10, with a uniform

470age of 96 weeks. Sciatic nerves served as the study tissue.

471**Figure 3. Immunohistochemical detection of MerTK expression in each group.** MerTK
472was expressed in all the groups and was significantly upregulated in the DPN group. Scale
473bars = 50 μ m. Rat counts per group were: CON: 14, CON+MRX-2843: 14, T2DM: 10, DPN:
47412, DPN+MRX-2843: 10, with all rats aged 96 weeks. The sciatic nerve was the tissue of
475interest.

476**Figure 4. Western blotting and ELISA detection of MerTK expression in each group.** (a)
477Immunoblotting images of MerTK are representative of each group. MerTK protein levels
478were detected in different groups using western blotting. Gene expression was normalized to
479the β -actin levels in each sample. (b) Serum MerTK levels were measured using ELISA. (c)
480Phosphorylated MerTK (p-MerTK) serum levels were also assessed via ELISA. * $p < 0.05$; ns
481= no statistical difference. Rat numbers were: CON: 14, CON+MRX-2843: 14, T2DM: 10,
482DPN: 12, DPN+MRX-2843: 10, all aged 96 weeks.

483**Figure 5. Levels of INS, TC, GHB, and TG in the serum.** (a) INS levels in each group. (b)
484TC levels in each group. (c) GHB levels in each group. (d) TG levels in each group. * $p <$
4850.05; ns, no statistical difference. Rat group counts were: CON: 14, CON+MRX-2843: 14,
486T2DM: 10, DPN: 12, DPN+MRX-2843: 10. Rats in all groups were 96 weeks old.

487**Figure 6. Structural changes of the sciatic nerve by the observation of light and electron**
488**microscope.** (a) The structure of the sciatic nerve was observed under light microscopes after
489the HE and TB staining respectively (scale bar = 50 μ m). (b) Structure of the sciatic nerve
490was observed under an electron microscope at magnification of 4000x, 8000x and 20000x.
491The rat group counts were: CON: 14, CON+MRX-2843: 14, T2DM: 10, DPN: 12,
492DPN+MRX-2843: 10, with each group's rats aged 96 weeks.

493**Figure 7. Immunohistochemical detection of NF- κ B (P65) expression level in each group.**
494P65 was expressed in all groups, and the expression of P65 was upregulated in the DPN
495group and further upregulated after MerTK inhibition. Scale bar = 50 μ m. Rat numbers per

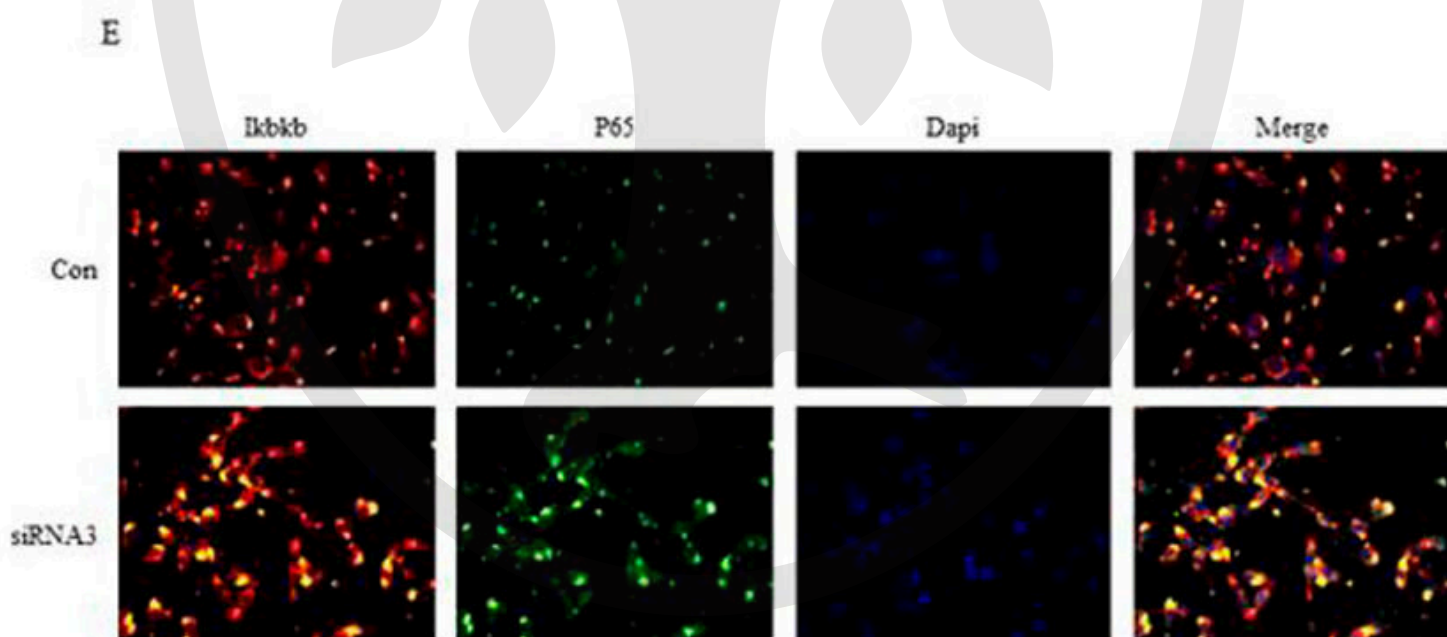
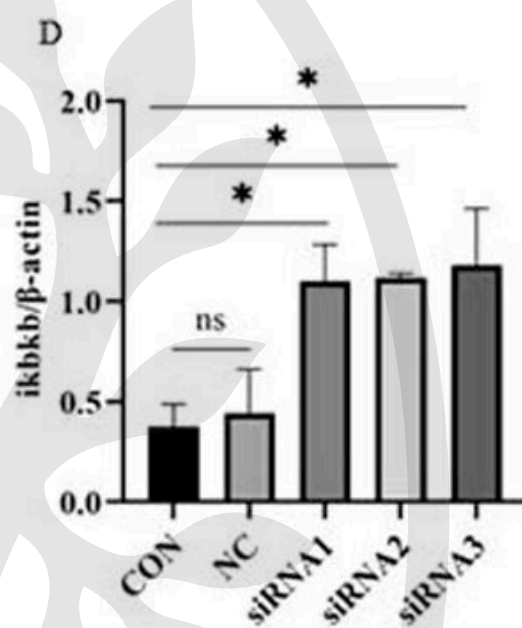
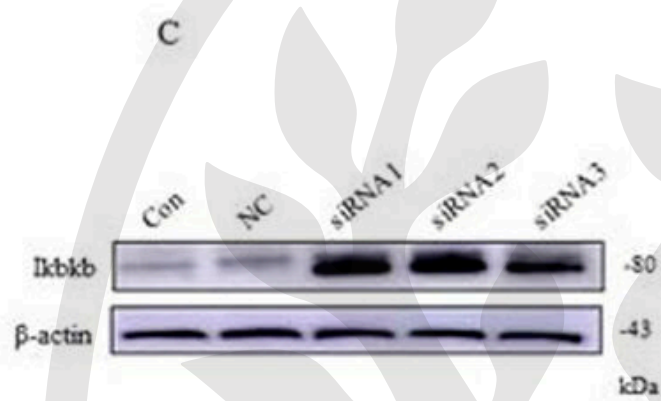
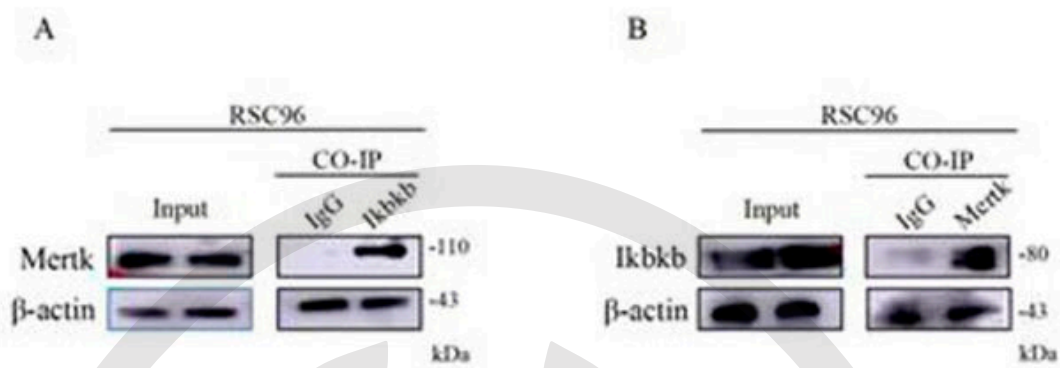
496group were: CON: 14, CON+MRX-2843: 14, T2DM: 10, DPN: 12, and DPN+MRX-2843:
49710, all aged 96 weeks. The sciatic nerve was selected as the study tissue.

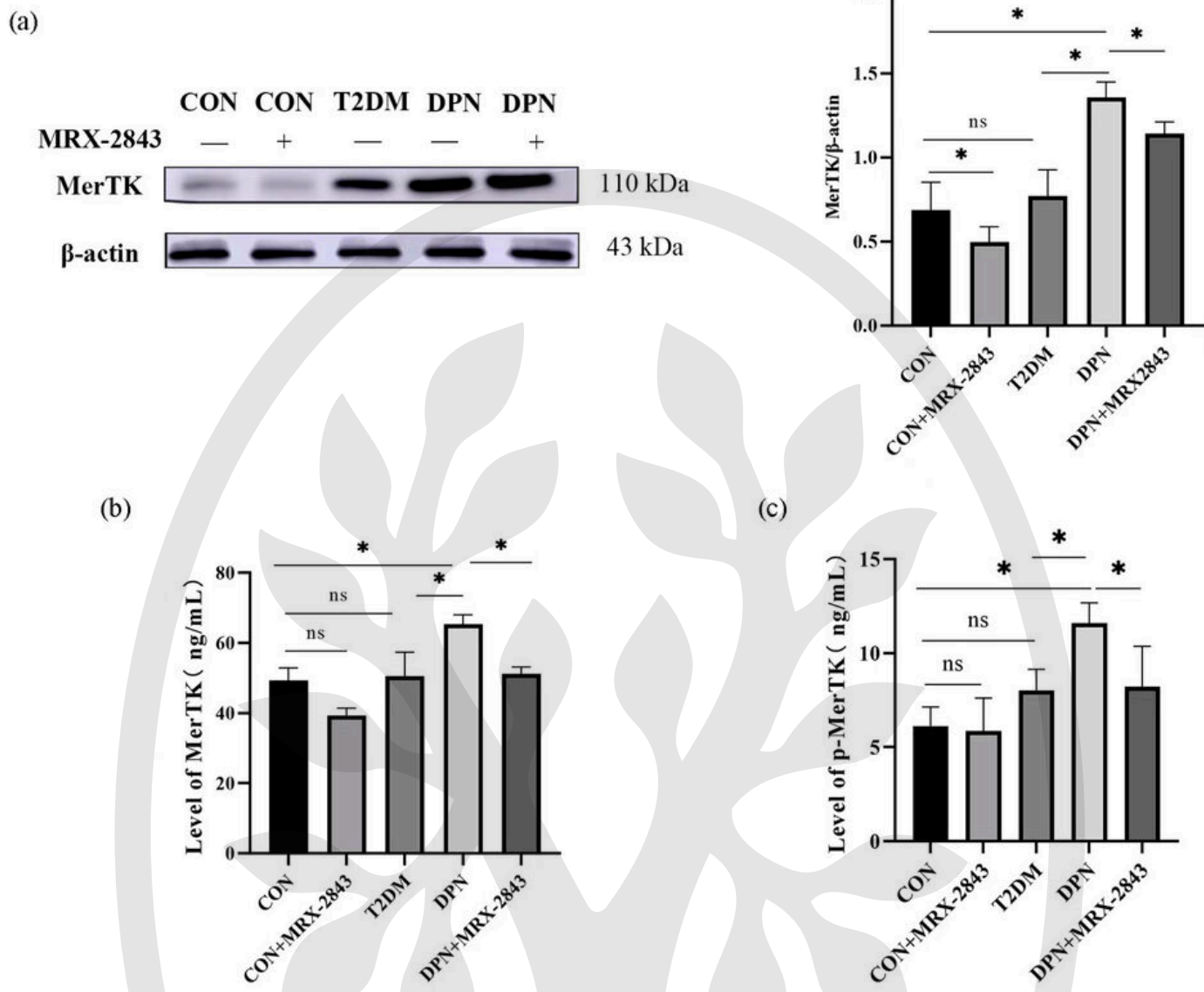
498**Figure 8. Western blotting detection of NF- κ B (P65) and TNF- α expression level in each**
499**group.** Immunoblotting images of P65 and TNF- α are representative of each group. The
500levels of proteins for P65 and TNF- α were detected in different groups by western blotting.
501Gene expression was normalized to the β -actin levels in each sample. * $p < 0.05$; ns, no
502statistical difference. Group rat numbers were: CON: 14, CON+MRX-2843: 14, T2DM: 10,
503DPN: 12, and DPN+MRX-2843: 10, with an age of 96 weeks for all rats. The sciatic nerve
504was the chosen tissue.

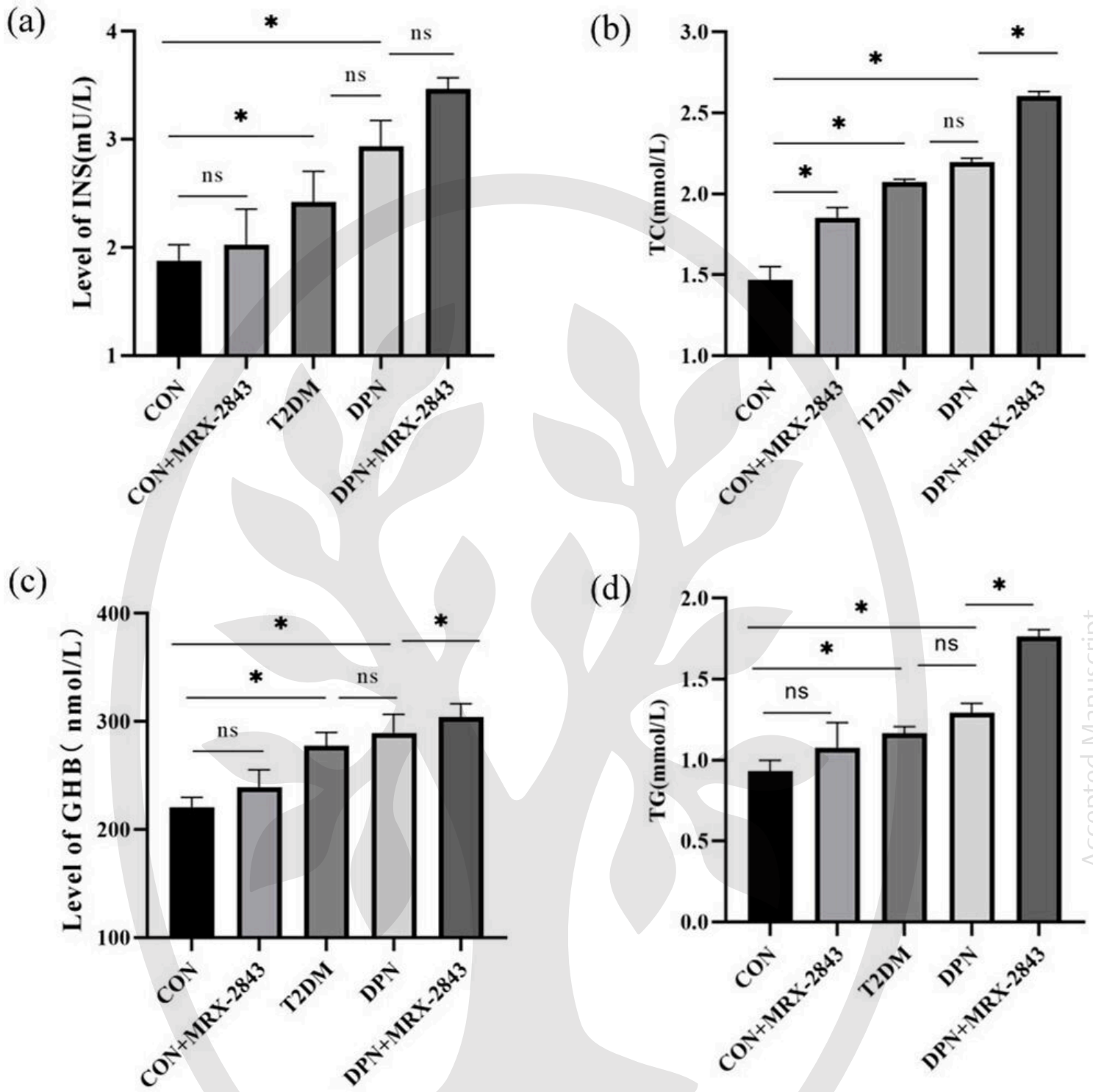
505**Figure 9. Levels of P65, TNF- α , and IL-1 β in the serum detected by ELISA.** (a) P65
506levels in each group. (b) TNF- α levels in each group. (c) IL-1 β levels in each group. * $p <$
5070.05; ns, no statistical difference. Rat counts for each group were: CON: 14, CON+MRX-
5082843: 14, T2DM: 10, DPN: 12, and DPN+MRX-2843: 10. All groups' rats were aged 96
509weeks.

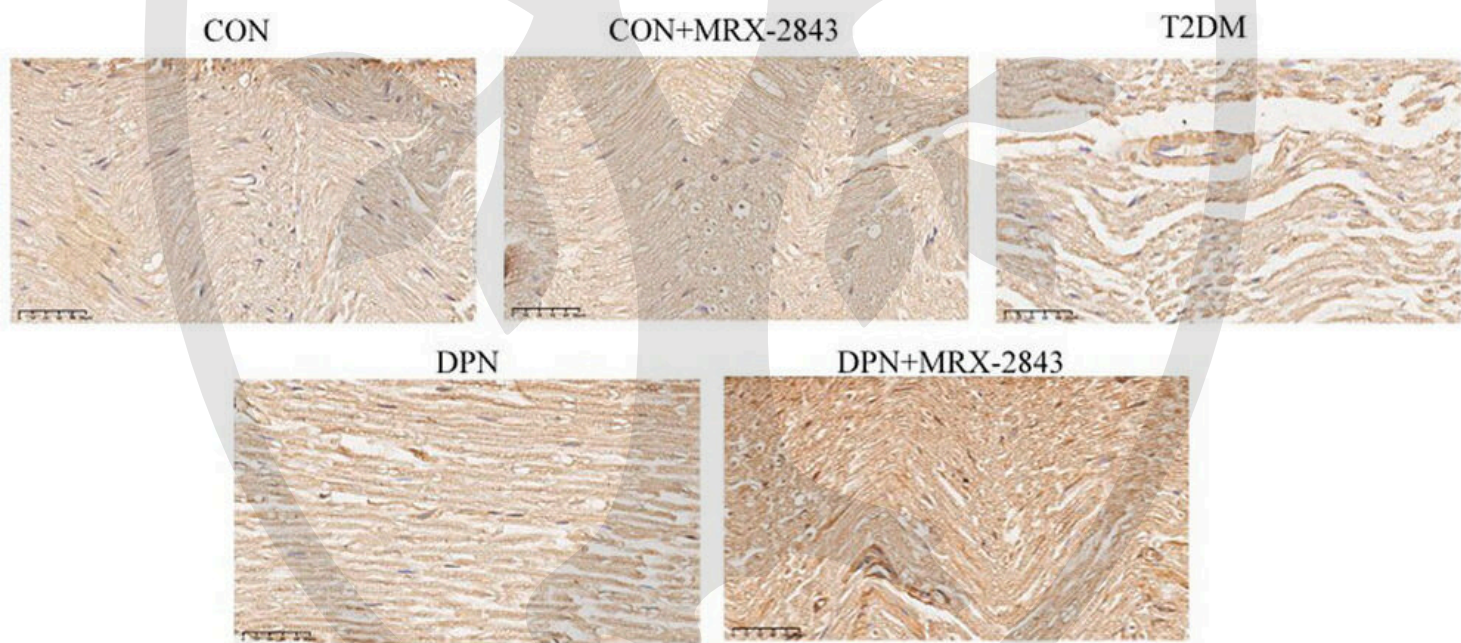
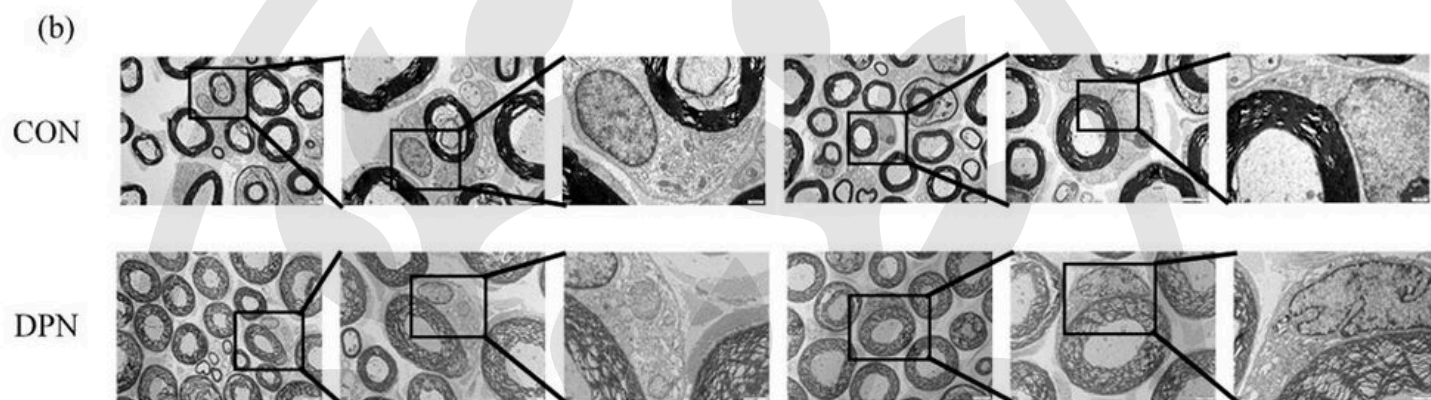
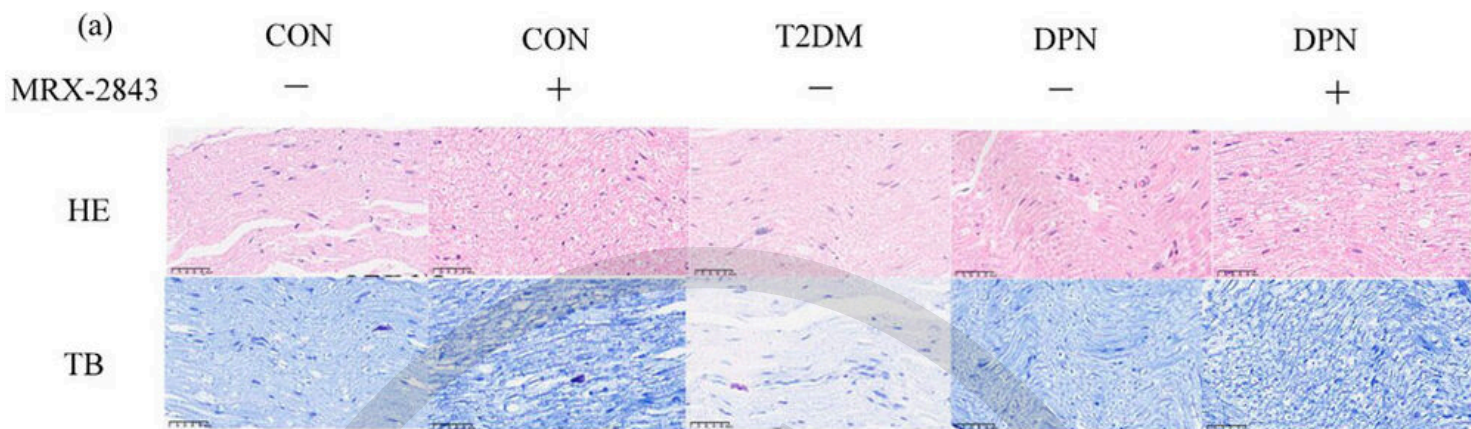
510**Figure 10. MerTK and I κ B κ B interaction in Schwann cells via immunoprecipitation**
511**assay.** (A) I κ B κ B immunoprecipitates were probed with MerTK antibody. (B) MerTK
512immunoprecipitates were probed with I κ B κ B antibody. "Input" signifies the positive control,
513while "IgG" marks the negative control. (C) I κ B κ B expression post-treatment with three
514MerTK siRNAs and a negative control agent (NC) was determined by western blot. (D)
515Protein levels of I κ B κ B across groups. (E) I κ B κ B and P65 expression post-MerTK-siRNA3
516treatment was observed through immunofluorescence (blue fluorescence: nuclei; red
517fluorescence: I κ B κ B; green fluorescence: P65).

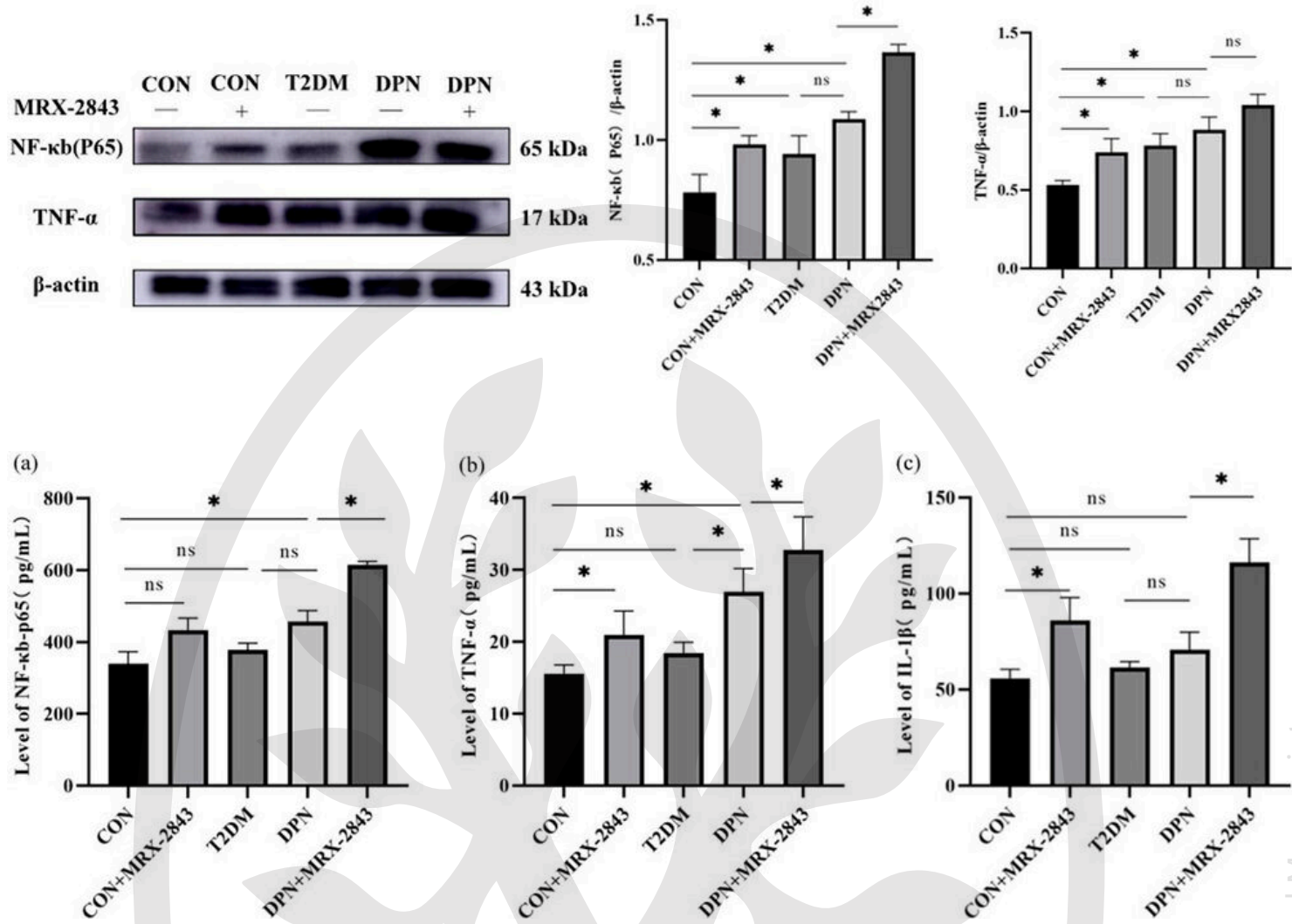
518

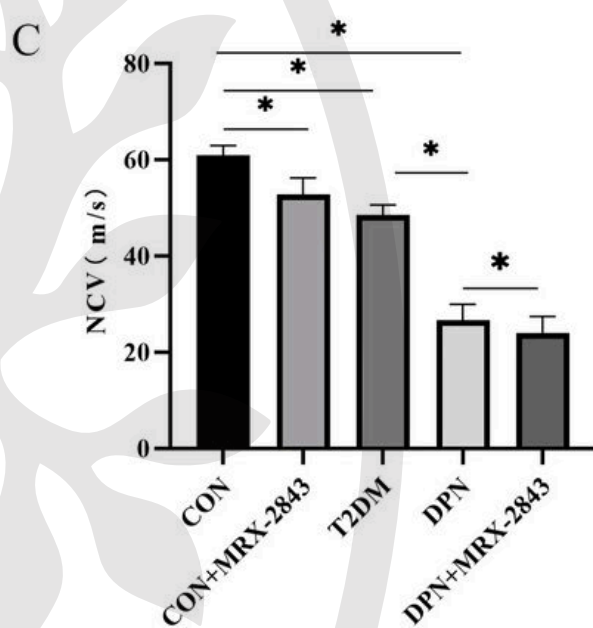
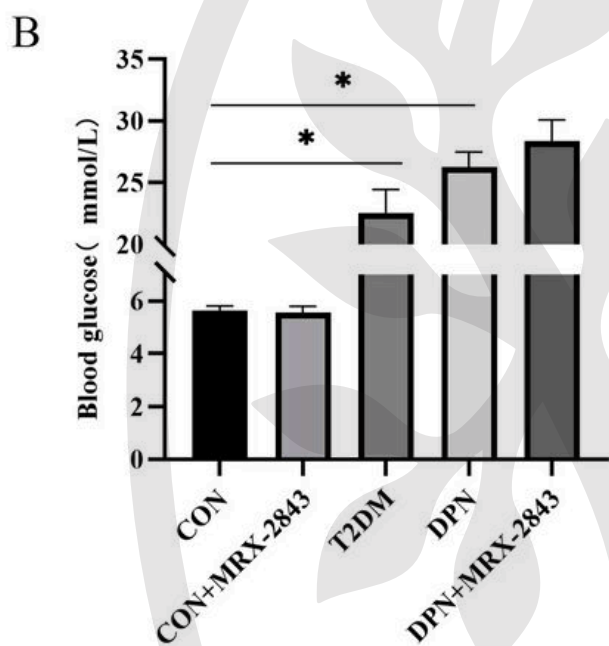
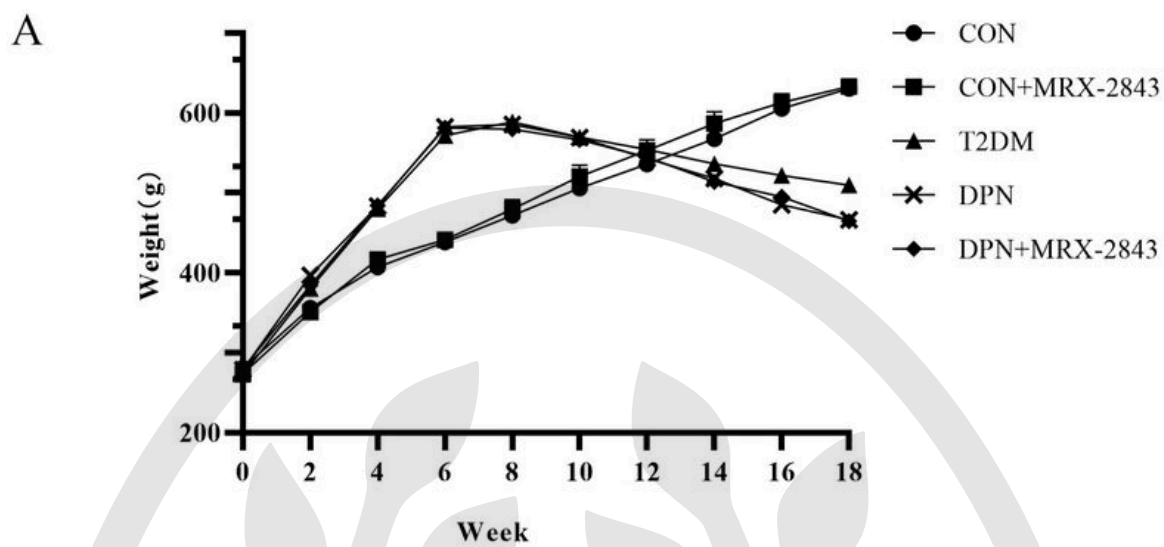


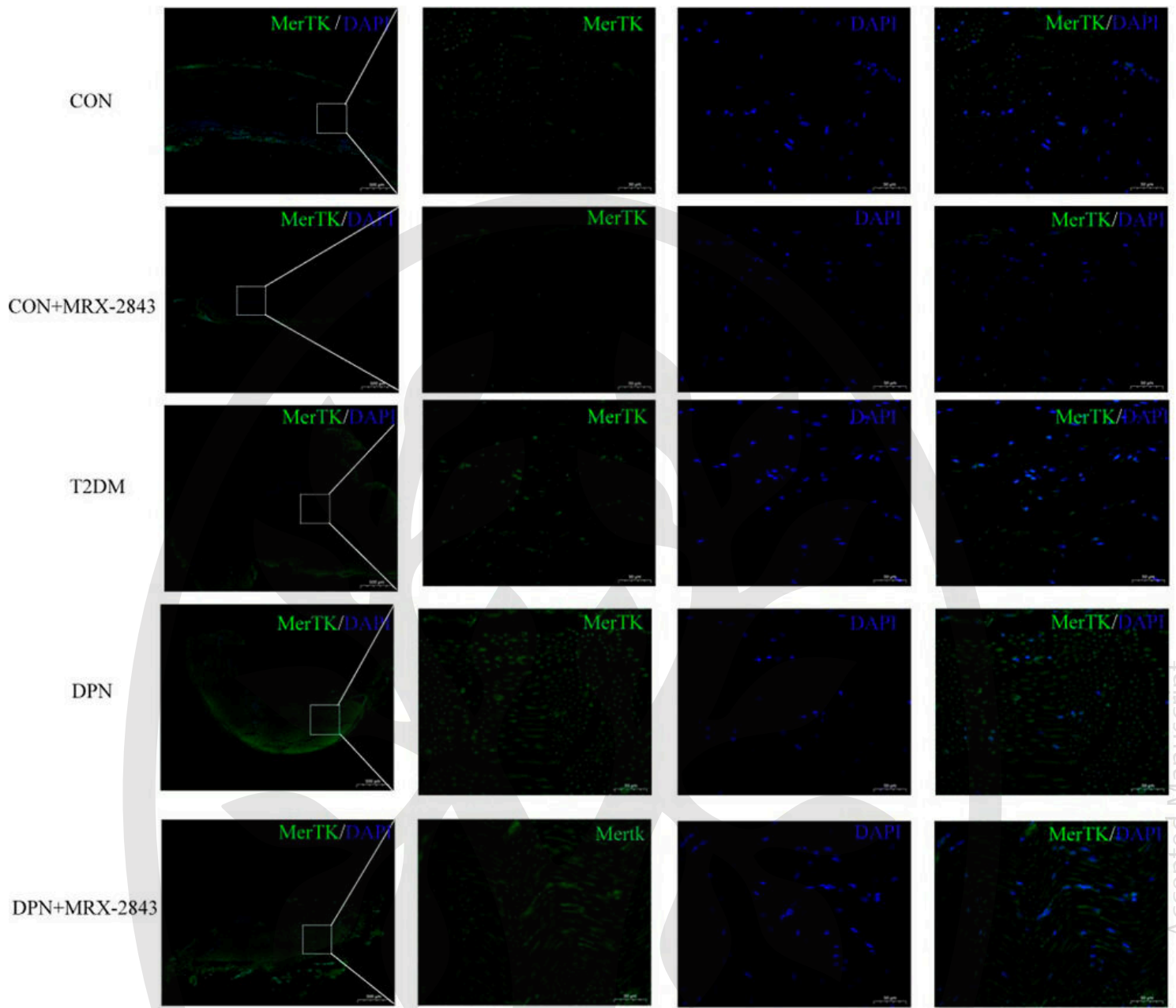




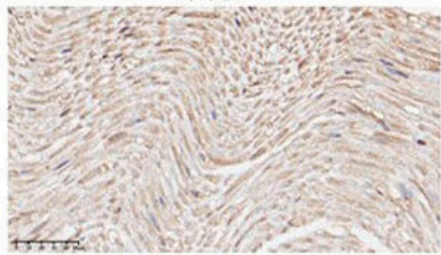




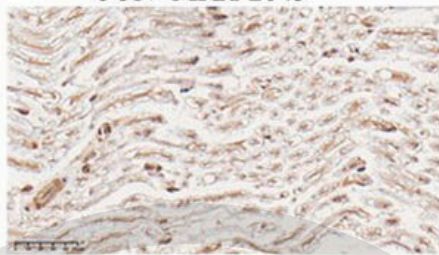




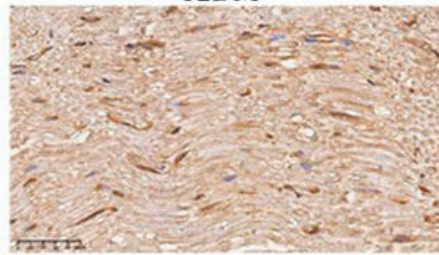
CON



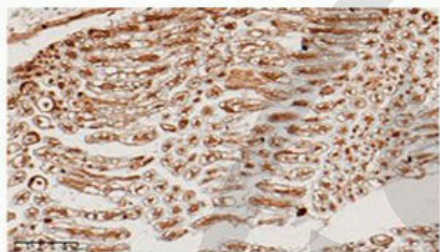
CON+MRX-2843



T2DM



DPN



DPN+MRX-2843

